WHITE DWARF – RED DWARF SYSTEMS RESOLVED WITH THE *HUBBLE SPACE TELESCOPE*: I. FIRST RESULTS

J. Farihi[1,2], D. W. Hoard[3,4], & S. Wachter[3]

jfarihi@gemini.edu,hoard@ipac.caltech.edu,wachter@ipac.caltech.edu

ABSTRACT

First results are presented for a *Hubble Space Telescope* Advanced Camera for Surveys snapshot study of white dwarfs with likely red dwarf companions. Of 48 targets observed and analyzed so far, 27 are totally or partially resolved into two or more components, while an additional 15 systems are almost certainly unresolved binaries. These results provide the first direct empirical evidence for a bimodal distribution of orbital separations among binary systems containing at least one white dwarf.

Subject headings: binaries: general—stars: fundamental parameters—stars: low-mass, brown dwarfs—stars: luminosity function, mass function—stars: formation—stars: evolution—white dwarfs

1. INTRODUCTION

The study of low mass stellar and substellar companions to white dwarfs yields useful information regarding the initial mass function near the bottom of the main sequence and below, the overall binary fraction of intermediate mass stars, and the long term stability and survivability of low mass objects in orbit about post-asymptotic giant branch stars (Zuckerman & Becklin 1987, 1992; Schultz et al. 1996; Green et al. 2000; Wachter et al. 2003; Farihi 2004; Farihi et al. 2005). Of particular interest is common envelope evolution and its consequences for any low mass companion. Understanding how low mass, unevolved companions fare inside and outside a common envelope is an easier task than distentangling

[1]Gemini Observatory, Northern Operations, 670 North A'ohoku Place, Hilo, HI 96720

[2]Department of Physics & Astronomy, University of California, 430 Portola Plaza, Los Angeles, CA 90095

[3]Spitzer Science Center, California Institute of Technology, MS 220-6, Pasadena, CA 91125

[4]Department of Physics & Astronomy, Pomona College, 610 North College Ave, Claremont, CA 91711

binaries which have experienced two envelopes, such as double degenerates, and should provide insight into more complex binary evolution.

This paper presents the first results from a *HST* Advanced Camera for Surveys (ACS) imaging survey of 90 candidate white dwarf + red dwarf binaries. The goals of the study are to empirically test the bimodal distribution of orbital semimajor axes predicted by post-asymptotic giant branch binary evolution models, and to examine the distribution of companion masses as a function of current separation (Jeans 1924; Bond 1985; Zuckerman & Becklin 1987; Valls-Gabaud 1988; Bond & Livio 1990; de Kool & Ritter 1993; Yungelson et al. 1993; Schultz et al. 1996; Livio 1996; Maxted et al. 1998; Schreiber & Gänsicke 2003; Farihi 2004).

2. PROGRAM DESCRIPTION

2.1. Primary Motivation

The prime focus of the present study is to image white dwarf + red dwarf pairs with sufficient spatial resolution to directly probe the $\sim 0.1-10$ AU range. Specifically, models of orbital expanion due to adiabatic mass loss, combined with models of frictional inspiral within a circumbinary envelope, predict a gap between diminished ($a \lesssim 0.1$ AU, $P \sim 10^{-2}-10^{-4}$ yr) and augmented ($a \gtrsim 5$ AU, $P \sim 10^{1}-10^{3}$ yr) orbits for low mass, unevolved companions to white dwarfs. A crude model of the expected distribution is given in Farihi (2004); basically, companions originally within $r = 2$ AU are brought inward of 0.1 AU, while those formerly outside this radius migrate farther by a factor of 3.

2.2. Sample Stars

The selected program stars, taken from and described in Wachter et al. (2003), are almost exclusively white dwarfs in McCook & Sion (1999) which were found by Wachter et al. (2003) to exhibit excess near-infrared emission in the 2MASS point source catalog (Cutri et al. 2003). Several additional targets of a similar nature were taken from Farihi (2004). White dwarfs with measured near-infrared flux above the photospheric contribution are strong candidates for harboring cool, low mass companions. With radii of $R \sim 1\ R_{Jupiter}$, low mass stellar and substellar companions to white dwarfs ($R \sim 1\ R_{\oplus}$) can easily dominate the spectral energy distribution of the binary at red to near-infrared wavelengths, despite their low luminosities and low effective temperatures (Probst 1983; Zuckerman & Becklin 1987,b, 1992; Green et al. 2000; Wachter et al. 2003; Farihi 2004; Farihi et al. 2005). The

target list for the white dwarfs discussed in this paper is given in Table 1.

2.3. Observations

The present data were taken with the ACS (Ford et al. 1998) High Resolution Channel (HRC) aboard *HST*. The observations at each target consisted of a small 4-point dither pattern with the F814W (approximately I band) filter to such a depth as to reach signal-to-noise (S/N) $\gtrsim$ 50 on both the white dwarf and its suspected red dwarf companion. These dithered frames were processed with MULTIDRIZZLE[1] to create a single combined, cosmic ray free image on which to perform astrometry and photometry.

2.4. Data Analysis

Each reduced image was visually inspected, and if two or more components were seen separated by $\gtrsim 0.''5$, or if the candidate binary appeared to be a single unresolved point source, the analysis was as follows. For these single or well resolved multiple point sources, astrometry and aperture photometry were performed with standard IRAF tasks. A few astrometric tasks were carried out with IDP3[2], which has the ability to determine the length and orientation of the major and minor axes in a gaussian profile fit. Both centroid and radial profile fits were executed for each star to determine its coordinates on the chip and to measure the full width at half maximum (FWHM), as well as eccentricity. Radial profiles were fit using a $0.''075$ (3 pixel) radius, while photometry was carried out with a $0.''125$ (5 pixel) aperture radius. Corrections to the standard ACS aperture, as well as appropriate sky annuli values, and color corrections, were taken from Sirianni et al. (2005). Counts were converted into flux, then into Vega magnitudes, and finally into Cousins I band magnitudes, all following the methods and calibrations of Sirianni et al. (2005).

If a binary appeared resolved but with point-spread functions (PSFs) separated by $\lesssim 0.''5$, then a different approach was used. In order to perform astrometry and photometry on these components with overlapping PSFs, it was first necessary to remove the nearby companion flux individually for each star. For this purpose, TinyTim[3] was used to generate ACS PSFs which were then processed with MULTIDRIZZLE. These multidrizzled PSFs

[1]http://stsdas.stsci.edu/multidrizzle/

[2]http://nicmos.as.arizona.edu/software/

[3]http://www.stsci.edu/software/tinytim/

were interpolated, scaled, and subtracted in turn from each star of the binary systems to isolate one star at a time. Each binary component was then examined in the same manner as for single sources and resolved components as described above. However, after companion removal there were often residuals still contaminating aperture photometry out to $r = 5$ pixels. For these close binary components, an aperture of $r = 2 - 3$ pixels was used and the measured flux was corrected to $r = 5$ pixels using aperture corrections derived from all well-separated single point source science targets in the data set.

2.5. PSF Subtraction

PSF subtraction was performed in the manner described above for all science target point sources to search for faint, close companions. In a typical PSF subtracted image, the residuals contain some small structure which is likely attributable to imperfections in the artificial, multidrizzled PSFs. Although the residuals were typically $< 2 - 3\%$ of the peak flux, this still might obscure any close companions at $\Delta m \gtrsim 4$ magnitudes. There is an ongoing effort to improve the PSF subtractions by: 1) performing the subtractions on the calibrated, flat fielded images and then multidrizzling the resultant images or; 2) using real ACS multidrizzled PSFs rather than artificial ones.

3. FIRST RESULTS

Table 1 lists all astrometry and photometry results for the 48 targets analyzed so far in the program. The table is organized so that the first line for a given target provides data on the white dwarf and subsequent lines are the companion data. The first column lists the white dwarf number from McCook & Sion (1999), and the second column lists an alternate name for the white dwarf or the companion name. The third column contains "Yes" if the components are totally or partially resolved in the ACS observation, or "No" if unresolved. The fourth column lists the FWHM in arcseconds for the Airy disk from gaussian profile fitting, and the fifth column lists the ratio of the major to minor axes of the profile fit. The sixth and seventh columns contain the separation in arcseconds and the position angle in degrees of the companion, if present. The eighth and ninth columns list the photometry, in Vega magnitudes, for the F814W filter and Cousins I band. The last column lists system specific notes.

3.1. Photometric & Astrometric Errors

There are a several sources of photometric and astrometric errors for the data shown in Table 1. First, there is the flux calibration error of the ACS/HRC instrument, which is 0.5% (Sirianni et al. 2005). Second, there is the uncertainty in performing photometry on targets within calibrated, multidrizzled images. For targets with no neighbors within 0.″5, the photometric uncertainty is essentially the inverse of the S/N, which is $\leq 4\%$ for all 75 photometric targets (i.e. all white dwarfs and companions), and $\leq 2\%$ for all but 9 sources. Third, there is the error introduced by transforming the flux in the F814W bandpass to the Cousins I band, which according to Sirianni et al. (2005) is no more than a few percent. Fourth, there is the error introduced when photometry was executed on a target with a close ($< 0.''5$) companion. After PSF subtraction, a few companion point sources retained a very small amount of residual flux which fell into the $r = 2 - 3$ pixel photometric aperture of the target star. This is smaller than $2 - 3\%$ of the subtracted target's peak flux (§2.4). Fifth, there is error introduced by using photometric apertures of $r = 2 - 3$ pixels which were then corrected to $r = 5$ pixels. The standard deviations in these correction factors were $1 - 3\%$, depending on aperture size and spectral type. The end result of adding all of these photometric errors in quadrature is that: typical errors for isolated point sources are $< 5\%$, while those for point sources with close companions are typically $< 6\%$.

Only relative astrometry between multiple system components has been perfomred in the study. The astrometric errors for point sources without close companions are completely due to the uncertainty in centroiding, which is strictly a function of S/N. These are typically ≤ 0.04 pixels (0.″0015 for S/N ≥ 50). For targets with close companions, the measured centroid can be biased in the direction of the companion, if its flux is not removed by PSF subtraction. Although the measured centroid uncertainty for these binary components had essentially the same range of errors as for single point sources, it is possible that small biases remained for targets contaminated by any positive or negative residual flux from its PSF-substracted close companion. Using $2 - 3$ pixel radii for centroiding and comparing the value obtained for a target with a close companion before and after PSF subtraction of the companion, shifts were measured that were no larger than 0.2 pixels (0.″005). The centroiding errors for components of close binaries are no larger than this shift.

3.2. Resolved Systems

As can be seen in Figures $1 - 5$ and Table 1, there are 28 systems for which 2 or more objects were totally or partially resolved (one of which is a previously known wide red dwarf companion that fell within the ACS field of view and was itself resolved into 2

close components). Generally speaking, the ACS multidrizzled PSFs at F814W had FWHMs $< 0.''077$ and were symmetric to within 5% of unity in the ratios of their major to minor axes by gaussian profile fits. This allowed mostly resolved binaries with clearly separated Airy disks to be imaged down to $0.''09$ in separation at $\Delta m = 1 - 2$ magnitudes between the components. For those binaries separated by $> 0.''4$ (17 in all), there was very little or no overlap between component PSFs, and both the white dwarfs and red dwarfs were used to derive aperture corrections to be used for more closely separated pairs.

It should be noted that there are a few resolved binaries at separations $> 2''$, which, in principle, would be resolvable from the ground with good seeing. The reason for this is that the sample was selected from unresolved 2MASS point sources, where the beam size is approximately $2''$ at J band in the images provided by the archive server. Typically, equally luminous binaries at magnitudes $J \approx 12 - 15$ mag can appear partially resolved in 2MASS at separations of $2 - 4''$ (Wachter et al. 2003). However, the fact that most red dwarfs in this sample are $2 - 3$ magnitudes brighter than their white dwarf primaries at J band makes it difficult or impossible to identify them as binaries in the 2MASS images.

3.3. Partially Resolved Systems

For imaged binaries separated by $< 0.''4$, there are two varieties: those in which two distinct Airy disks are present and those in which there is a single, elongated Airy disk. Pairs with two distinct PSF cores were treated as described above, while those with elongated cores proved problematic during PSF fitting and subtraction aimed at revealing individual point sources. Relative to the apparently single stars in the ACS image set, these closest binaries all display significantly larger than normal residuals after single PSF subtractions are performed, corroborating their binarity.

There are three systems (0949+451, 1419+576, 1631+781) whose images show the presence of binaries with likely separations $< 0.''025$, corresponding to a single ACS/HRC pixel. In all three cases, the elongated Airy disk is associated with the red dwarf component of a resolved binary; i.e., these systems are all triples. This is a fortunate situation because in each case the white dwarf component can be used as a comparison PSF. These systems are described in §3.7.

The separations of these very close binary systems were estimated in the following manner. All the measured PSFs in Table 1 show some very minor elongation that is typically on the order of one milliarcsecond. Specifically, the difference between the major and minor axes of the gaussian profile fits is typically $\lesssim 1 - 2$ mas. For the three close doubles, these

differences, or elongations, lie in the range $7 - 9$ mas. Equally luminous components were assumed and the separation of the binary was taken to be its elongation. Of course, if the pair is not equally bright, then the separation will be slightly larger, but contour plots of all three objects display a high degree of symmetry along the major axes, consistent with equal luminosity.

Without spatially resolved spectra of the close binary components of these triple systems, it cannot be firmly concluded that all three are double red dwarfs. It is likely that only one of the systems will be observable from the ground as a spectroscopic target that is spatially resolved from its white dwarf primary. Therefore, it may be difficult (or impossible) to know with certainty the nature of the two close components in the remaining two systems. However, depending on the actual orbital period, it may be possible with radial velocity monitoring to confirm the nature of these candidate double red dwarfs from the ground over a period of one to a few years. None of the other 24 spatially resolved white dwarf + red dwarf pairs have separations as small as the three targets with elongated Airy disks, and it is a safe assumption (for reasons discussed in §4) that these are double red dwarfs.

3.4. Unresolved Systems

There are 15 systems in Table 1 for which there is strong photometric evidence, and often spectroscopic evidence, for the presence of an unresolved white dwarf + red dwarf pair. In fact, a thorough literature search beyond McCook & Sion (1999) reveals that a few of these systems are recently (since their selection as targets for this program) discovered DA+dMe systems, radial velocity variables, or low mass (He core, $M < 0.45\ M_{\odot}$) white dwarfs – all of which imply binaries with separations $\lesssim 0.1$ AU (Saffer et al. 1993; Marsh et al. 1995; Schmidt et al. 1995; Schultz et al. 1996), consistent with single point sources in the ACS observations. In any case, all of these stars have composite optical and near-infrared colors perfectly consistent with white dwarf and red dwarf components (Wachter et al. 2003).

For these binaries, it was necessary to calculate the flux contribution of the white dwarf in order to subtract it and obtain the flux of the red dwarf companion. This was done utilizing techniques discussed in Farihi (2004) and Farihi et al. (2005), and §3.6, where particular attention was given to avoid biasing the calculations by excluding white dwarf data which may have been contaminated by the cool companion star.

There were 6 targets (§3.7) for which the evidence of binarity was based on low S/N (< 7 or < 5) K_s data in the 2MASS point source catalog. These were included in the HST/ACS survey as low priority targets and do not belong to the sample of highly probable

white dwarf + red dwarf binaries. As yet, none of these targets have revealed companions in the ACS observations.

3.5. Establishing Physical Multiplicity

Any study of stellar multiplicity must address the likelihood of physical association between putative companions. There are several reasons why all the targets designated here as multiples have a very high probability of being gravitationally bound. The first and foremost is spatial proximity – the white dwarf targets are associated with a single point source in 2MASS images. Second, the combination of optical and near-infrared colors yields photometric distance ranges for each component that overlap when appropriate, mundane white dwarf and red dwarf stellar parameters are assumed. Third, some of the systems imaged in this study have published references listed in Tables $1-4$ containing spectroscopic confirmation of their red dwarf companions in unresolved, composite observations, and/or previously established common proper motion. Fourth, common proper motion is almost certain for all posited multiples over the timescales since the identification of the white dwarf component $20-50$ years ago; otherwise any false pairs should separate when "blinking" images available through the Digitized Sky Survey (e.g., in the northern hemisphere, the first and second epoch Palomar Observatory Sky Survey plates). Fifth, there exist several white dwarf + red dwarf studies which have established spectroscopic and/or common proper motion confirmation for numerous targets of a nearly identical nature (Schultz et al. 1996; Raymond et al. 2003; Farihi 2004; Farihi et al. 2005). Therefore, the multiple stellar systems presented here should be regarded as physically associated until shown otherwise.

3.6. Spectral Type Constraints & Component Identification

To determine the projected companion separations in astronomical units, distances to each binary had to be assessed. Table 2 lists the stellar parameters from the literature for the white dwarf primaries in Table 1. The first column contains the white dwarf number, followed by effective temperature, surface gravity, apparent visual magnitude, photometric distance, and references. A single digit following the decimal place for $\log g$ indicates an assumption of $M = 0.60\ M_{\odot}$. The V magnitude is either a value uncontaminated by the red dwarf or one derived (based on effective temperature and models, magnitudes and colors in other filters, or photographic magnitudes and colors; Farihi 2004; Farihi et al. 2005) to more correctly reflect the likely uncontaminated value. Distances were calculated from absolute magnitudes for individual white dwarfs, using the models of Bergeron et al. (1995a,b) as well

as specified references in Table 2.

Less than half of the white dwarf targets in Table 2 have well-determined stellar parameters (i.e., $T_{\rm eff}$, $\log g$) in the literature and, hence, fairly reliable distance estimates. For these well-studied white dwarfs there are published parameters based on data (typically spectra, but also photometry where available) and analyses which are not contaminated or biased by the light from their red dwarf companions. Fortunately, most if not all ground-based white dwarf studies are performed in the $3000-6000$ Å range, where most red dwarfs should not contribute significantly. However, there are plenty of cases where flux is seen at these wavelengths and this has been taken into account in Table 2 and often by authors in the corresponding references.

For the remainder of the targets, published white dwarf parameters do not exist at present; McCook & Sion (1999 and references therein) sometimes contain UBV or other optical photometry, but frequently there is only a single photographic magnitude and/or a spectral type with no temperature index. Therefore, at worst, the values in Table 2 represent conservative best guesses – assuming parameters which would make the white dwarf and any companion typical – but more often they are guesses informed by available data. Some of the ways in which the effective temperatures and visual magnitudes were estimated for white dwarf targets include: (1) published $U-B$ color, which is unlikely to be contaminated by a cool companion; (2) the implied color indices (e.g., $B-I$) for any white dwarf which was resolved from its companion in the ACS observations; (3) information on the colors and spectral type of the companion star from 2MASS data, ACS photometry, or other literature sources; (4) any published optical spectrum revealing one or both of the binary components (but without parameter determinations).

Generally, for each target all available information was gleaned from the USNO-B1.0 (Monet et al. 2003), 2MASS All-Sky Point Source (Cutri et al. 2003), and SuperCOSMOS Sky Survey catalogs (Hambly et al. 2001) to assist in constraining and disentangling binary component stellar parameters. Although photographic photometry can have large absolute calibration errors, typically ~ 0.3 mag, resultant colors tend to be as accurate as $\lesssim 0.1$ mag for the magnitude range spanned by the white dwarf targets here (Hambly et al. 2001) and can be useful in a number of ways. Any colors assist in the assessment of where the flux of the red dwarf begins to dominate the spectral energy distribution of the binary, which is typically shortward of 8000 Å. If published optical photometry or spectra were suspected of contamination (i.e., effective temperature underestimated in the literature) then adjustments using model colors based on a more likely (conservative) temperature were made. In this way, the best available data and estimates were used for all targets in order to constrain white dwarf parameters and subsequently deconvolve any composite $IJHK$ data to obtain

colors and magnitudes for red dwarf companions, following methods described fully in Farihi (2004) and Farihi et al. (2005). Where model white dwarf parameters were needed, they were taken from Bergeron et al. (1995a,b) and P. Bergeron (2002, private communication). Where empirical red dwarf parameters were needed, they were taken from Kirkpatrick & McCarthy (1994) and Dahn et al. (2002).

A separate but related issue is the identification of the hot and cool components for the numerous binaries resolved in the ACS observations. Utilizing techniques discussed above, and because in almost every case there was a significant brightness difference ($\Delta m \gtrsim 1$ mag) between the components, there is high confidence that the white dwarf component was correctly identified in the ACS images (possible exceptions are discussed in §3.7). Specifically, the implied $I-K$ color of the red dwarf and the $V-I$ color of the white dwarf are consistent only if the components were correctly identified; reversing identities leads to contradictions. Additionally, the ACS camera scatters light at red wavelengths, yielding significant haloes for all bright objects (see Figure 5 of Sirianni et al. 2005), and broadening the PSF of any red objects relative to blue objects (Sirianni et al. 2005). The measured PSF sizes in Table 1 reflect this phenomenon, with a single possible exception discussed in §3.7. Despite apparent good agreement and reassurance that the individual components have been correctly identified, it is by no means absolute. In a few cases, it is possible that an apparently single, resolved binary component is itself an unresolved double red dwarf binary or white dwarf + red dwarf binary.

Tables 3 and 4 list the measured and derived parameters of the red dwarf companion stars. In the first column is the white dwarf number followed by the companion name. The third column contains the spectral type estimate based on the $I-K$ color listed in the fourth column. The fifth column lists the photometric distance to the red dwarf based on empirical M dwarf data (Kirkpatrick & McCarthy 1994; Dahn et al. 2002). It should be mentioned that the white dwarf distance estimates listed in Table 2 do not always agree with the implied distance to the red dwarf from absolute magnitude-spectral type relations (Farihi 2004; Farihi et al. 2005). There are several reasons why this might happen: (1) the white dwarf has a mass significantly above or below the typically assumed 0.60 $M_{\odot}$ value for field DA stars; (2) the effective temperature of the white dwarf has been poorly estimated; (3) the spectral type of the red dwarf has been poorly estimated; (4) either the white dwarf or red dwarf is itself an unresolved binary; (5) the intrinsic width of the lower main sequence in a Hertzsprung-Russell (or reduced proper motion) diagram is at least ± 1 magnitude, the slope is steep, and placement of a component depends upon both metallicity and age. This alone can impose on the order of $1-2$ magnitudes of apparent discrepancy with the white dwarf estimate when photometric distances are all that is available. These are some of the reasons why spectral type estimation was based on color, not on any absolute magnitude

implied by the (often nominal) photometric distance to the white dwarf (Farihi 2004; Farihi et al. 2005).

In principle, obtaining a good photometric distance to nearly all the white dwarfs in the sample is feasible, since the bulk are DA white dwarfs which can be spectroscopically fit sans contamination (by avoidance if necessary) in the $3000 - 5000$ Å region for $T_{\rm eff}$ and log g. However, a similar spectroscopic assessment is not possible for the red dwarf secondaries; spectral types can be determined to limited accuracy by subtracting the expected white dwarf contribution over $6000 - 10000$ Å, but the equivalent of a stellar radius (log g) determination does not exist. Using empirical absolute magnitude-spectral type relations is likely to prove reliable in most cases (assuming knowledge of an accurate spectral type); however, there is intrinsic scatter in absolute magnitudes for a given red dwarf spectral type, potentially compounded up to $\sim 1 - 2$ magnitudes by metallicity and/or multiplicity (Gizis 1997; Reid & Hawley 2000; Farihi 2004; Farihi et al. 2005). For comparison and completeness, the red dwarf distance from color-magnitude relations is also listed in the tables.

3.7. Notes on Individual Objects

0023+388 is more likely closer to $d \approx 60$ pc than 24 pc as suggested by references in McCook & Sion (1999). The distance underestimate is likely due to the unresolved red dwarf causing the white dwarf to appear redder, cooler and, hence, nearer (Farihi 2004).

0131−163 is a singular case in which it was difficult to distinguish which resolved star is the white dwarf or red dwarf. The parameters in Table 3 present the most consistent scenario, but a full optical spectrum and multiband photometry should be able to reveal which star contributes more flux around 8000 Å.

0208−153 is the only resolved pair in which the PSF widths do not follow the pattern of $\theta_{rd} > \theta_{wd}$. The reason for this is unclear, but given the fact that ACS scatters more light for redder objects, this white dwarf could conceivably harbor an unresolved red companion.

0237+115, 0347−137, 1218+497, 1333+005, and *1458+171* all appear to have discrepancies betwen the distances implied by the (sometimes inferred) brightness of the white dwarf and red dwarf binary components. Many of the white dwarfs have reliable log g determinations (Dreizler & Werner 1996; Koester et al. 2001; Liebert et al. 2005) but the cool companion appears too bright for its color and, hence, may be a binary. In other cases, the white dwarf may be overluminous (or the red dwarf may be underluminous). These cases are those that stand out presently, but spectroscopic observations (which are currently being obtained) may resolve them.

0324+738 has many measurements in McCook & Sion (1999) and the current online version of that catalog that are either contaminated by nearby background stars or were performed on the wrong stars. Recently published values of $T_{\rm eff} = 4650$ K and an extremely low mass (Bergeron et al. 2001) are also likely due to the same phenomenon, as the white dwarf is currently moving between two background stars and has a nearby ($a \approx 13''$) red dwarf common proper motion companion (which is incorrectly identified as the white dwarf by coordinates in McCook & Sion 1999 and finder charts provided in the current online version of that catalog). These four stars are all currently within a $7''$ radius of one another. For the present work, the correct stars were identified by using Digitized Sky Survey images to confirm the pair by their common proper motion over 40 years and by their photographic magnitudes, colors and positions in the USNO-A2.0, USNO-B1.0, and 2MASS catalogs (Monet et al. 1998, 2003; Cutri et al. 2003). From the ACS images, the white dwarf has coordinates of $03^{\rm h}30^{\rm m}13.89^{\rm s}, +74°01'57.''1$ while the brighter component of the double red dwarf (resolved in the observations) is located at $03^{\rm h}30^{\rm m}14.37^{\rm s}, +74°02'09.''7$, both epoch 2005.09. Using Greenstein (1986) and the ACS data gives $V - I \approx 0.24$ for the white dwarf and (if correct) together with its measured parallax of $\pi = 0.''025$ would give $T_{\rm eff} \approx 9000$ K and $\log g \approx 8.74$ ($M \approx 1.05\ M_{\odot}$). The properly identified white dwarf does not have any published, accurate, and uncontaminated near-infrared data and, hence, there is currently no evidence for any close (i.e. unresolved by ACS), cool companion.

1133+489 is the same object as SDSS J113609.59+484318.9 for which van den Besselaar et al. (2005) recently determined that the white dwarf is a DB star with $T_{\rm eff} > 38,000$ K, despite the presence of He II absorption at 4686 Å in their spectrum, together with an M6 or later companion. The white dwarf was found to be a composite white dwarf by Greenstein (1986) and Wesemael et al. (1985) who correctly determined the primary to be a type DO star with $T_{\rm eff} = 47,500$ K plus a cool companion. However, a companion as late as M6 would place this system at a distance of about 166 pc based on JHK_s from 2MASS, implying $M_V = 11$ mag for the white dwarf and a mass $> 1.2\ M_{\odot}$. The present analysis finds the $I - K$ color of the companion gives a spectral type of M5, consistent if the white dwarf has $\log g \approx 8.3$ ($M \approx 0.84\ M_{\odot}$).

1247+550, 2211+372, 2323+256, and *2349−283* are all low priority targets whose 2MASS photometry in the Second Incremental Data Release, despite low S/N at K_s, suggested near-infrared excess (Wachter et al. 2003). Some of these targets have JHK_s data in the All Sky Point Source Catalog which differ significantly from the preceeding catalog values (Cutri et al. 2003). None of these white dwarfs show any evidence of companions in the ACS images, and until more accurate near-infrared photometry is available, binarity should be considered unlikely.

1517+502 is a rare DA+dC (white dwarf + dwarf carbon star) system (Liebert et al. 1994) which remained unresolved in the ACS observation. The expected magnitude difference at I band is 1.05 mag; thus, conservatively speaking, a separation of $\gtrsim 0.''05$ (≈ 20 AU) can likely be ruled out.

1603+125 is listed in McCook & Sion (1999) as a possible magnetic white dwarf, type DAH. Based on the deconvolved, $I - K = 1.38$, color for the companion, a spectral type of K3 is inferred. This places the system at $d \approx 1660$ pc and implies that the primary is very likely an sdB star with $M_V \approx 4.5$ mag (Maxted et al. 2000).

1619+525 displays three objects within a $3''$ radius on the ACS images; their separations and magnitudes are listed in Table 1. The photometry was performed with color and aperture corrections appropriate for one white dwarf and two red dwarfs of the implied intrinsic faintness and color. If this is a physical triple, then the ratio of the projected separations is 5.6 to 1. The companionship of the two brighter stars is quite firm as the elongated pair can be seen on at least 2 Digitized Sky Survey images, almost certainly comoving over 43 years. The third candidate companion lies within $0.''5$ of the white dwarf, which is located at $|b| = 43.9°$. Hence, they are quite likely to be physically associated. Additionally, the candidate third component appears quite red, as would be expected of a late M dwarf; the 2MASS images are elongated at JH, and especially at K_s, along the correct position angle. This is consistent if the tertiary candidate is a companion because, although the brightness difference of the two red dwarfs is 2.8 magnitudes at I band, it should become < 2 magnitudes in the near-infrared if the two contributing components are around M5 and DA2.8+M7 (Kirkpatrick & McCarthy 1994; Dahn et al. 2002). Attempts to deconvolve the 2MASS magnitudes into two components failed, however, and the 2MASS photometry may be inaccurate due to the presence of two objects (the white dwarf should contribute very little in the near-infrared). Ground-based followup should conclusively demonstrate that this system is a DA2.8+dM5+dM7 (approximate M types) triple system.

1631+781 is a triple system with a well-resolved red dwarf companion which is itself a barely resolved double. This system is mentioned in 47 papers in the literature since its discovery by Cooke et al. (1992), at least 12 of which mention or discuss its nature as a precatacylsmic variable or post-common envelope binary. However, both Sion et al. (1995) and Schultz et al. (1996) demonstrated the unlikelihood that the main binary lies in a close orbit by finding an absence of radial velocity variability in the Balmer emission lines from the companion. Catalán et al. (1995) added the possibility that the system is face on or has low enough inclination to preclude significant variations in radial velocity as seen from Earth. Bleach et al. (2002) conclude that the system is not face on from a positive detection of rotational broadening ($v_{rot} \sin i = 25.2 \pm 2.3$ km s^{-1}) in the red dwarf at several lines

in a high resolution optical spectrum. Given that all components of the triple system are seen in the ACS image, it is entirely possible that this system has a low inclination, and the line broadening reported by Bleach et al. (2002) might be due in part or in whole to the binarity of the red dwarf component. Somewhat surprisingly, Morales-Rueda et al. (2005) lists this system among all known detached, post-common envelope binaries with known periods, citing Fuhrmeister & Schmitt (2003) who report x-ray variability with a period of 69.4 ± 8.3 hours and a false-alarm probability of 4.4%. Since the main binary is quite widely separated, the source of the x-ray variations are either intrinsic to the hot degenerate star itself (i.e., perhaps a starspot) as seen in other single white dwarfs (Fuhrmeister & Schmitt 2003), or flare activity from one or both components of the red dwarf pair (Reid & Hawley 2000). In any case, two things are clear from the ACS data. First, this system never shared a common envelope, as the current projected separation of the double red dwarf from the primary is 17 AU ($P \geq 57$ years). Second, all the documented optical emission features arise from activity within the double red dwarf system, either intrinsic to one or both of the stars (interactions are unlikely at $a \gtrsim 0.4$ AU, $P \approx 100$ days).

1845+683 is a hot white dwarf ($V \approx 15.5$ mag, $T_{\rm eff} \approx 37,000$ K; see references in Table 2) reported as a binary in both Green et al. (2000) and Holberg et al. (2003). It is likely that the second reference is merely pointing to the work presented in the first reference, as there exists no other discoverable discussion of suspected binarity of this white dwarf in the literature. The 2MASS catalog gives $J = 16.07 \pm 0.09$ mag, $H = 16.28 \pm 0.22$ mag, and an upper limit of $K_s > 15.29$ mag for the white dwarf, which are consistent with a single star of the appropriate effective temperature, and also consistent with the ACS I band magnitude. Green et al. (2000) have $J = 14.85 \pm 0.10$ mag and $K = 14.37 \pm 0.19$ mag which apparently corresponds to a field star located $46''$ away at PA = 225°, which has 2MASS photometry of $J = 14.93 \pm 0.04$ mag, $H = 14.36 \pm 0.04$ mag, and $K_s = 14.30 \pm 0.09$ mag, all with S/N > 12. All this suggests that the white dwarf is neither a suspected nor confirmed binary.

2151−015 contains a resolved M8 dwarf, the coolest companion resolved in the survey so far. The identity of the white dwarf and red dwarf components are firm from ground-based $BVRI$ images, where the M star is seen partially resolved only at I (Farihi 2004; Farihi et al. 2005). However, the white dwarf exhibits a significant halo in the ACS image which is unexpected for a ~ 8500 K object, and not seen in other white dwarf primaries – even those with unresolved, spectroscopically confirmed, late M dwarf companions such as 0354+463 (Rubin 80, DA6+dM7; Farihi 2004; Farihi et al. 2005). While this may simply be the result of the fact that the primary is relatively bright compared to the other resolved white dwarfs, it might be due to a third, unresolved, even cooler component.

4. CONCLUSIONS

This HST/ACS survey was specifically designed to search for white dwarf + red dwarf binaries separated by around one to a few AU. Theory predicts, and extant observations support, a bimodal distribution of orbital separations in which low mass companions vacate this region during the post-main sequence evolution of the white dwarf progenitor (Jeans 1924; Bond 1985; Zuckerman & Becklin 1987; Valls-Gabaud 1988; Bond & Livio 1990; de Kool & Ritter 1993; Yungelson et al. 1993; Schultz et al. 1996; Livio 1996; Maxted et al. 1998; Schreiber & Gänsicke 2003; Farihi 2004). Specifically, companions within a few AU should interact both directly and tidally with the AGB slow wind and expanding photosphere, imparting some of their angular momentum to the envelope and arriving eventually at closer orbital semimajor axes. Those companions originally outside of a few AU should eschew the AGB envelope and experience an expansion of their orbital semimajor axes by a factor proportional to the total amount of mass lost There is no a priori reason to believe that the phase space around $\sim 0.5 - 5$ AU should be utterly devoid of low mass main sequence companions to white dwarfs. In fact, there should be some real width in both peaks of the actual bimodal distribution of separations, each with tails overlapping the "forbidden" range of semimajor axes.

Figure 2 displays the sensitivity of the survey to companions in the few AU range. Here, two assumptions are used; 1) $0.''010$ sensitivity, for companions at $\Delta m \lesssim 0.5$ mag and 2) $0.''025$ sensitivity, for companions at $\Delta m \lesssim 2$ mag. These assumptions are conservative, especially given the performed PSF subtractions. All targetted binary candidates are expected to have flux ratios corresponding $\Delta m < 2.5$ mag in the F814W filter. Figure 3 shows the distribution of projected separations for detected companions and upper limits for unresolved binaries.

So far, no white dwarf + red dwarf systems have been resolved at separations around a few AU. The ability of this survey to detect binaries of comparable luminosity at such separations is demonstrated by both Figures 2 and 3, plus the three very close binaries (likely double red dwarfs) in Table 5, implying that pairs separated by as little as 1 AU at $d = 100$ pc were at least partially resolvable. Although accurate distances are needed for the sample stars to confirm these preliminary findings, there are not yet any ambiguous cases where a reasonable change in the distance to the binary would bring the separation into the few AU range.

If these initial conclusions are correct, these data are the first empirical evidence for the bimodal distribution of low mass, unevolved companions to white dwarfs. This would also imply that as many as 100% of the 15 unresolved white dwarf + red dwarf pairs are in close orbits, and good candidates for radial velocity variables. If the first half of this survey is

representative of the whole, it should be expected that this program will eventually resolve around 55 total wide binaries, and identify around 30 total binaries that are candidate radial velocity variables.

5. FUTURE WORK

Followup work is currently being carried out for all program stars for which a good photometric distance determination (i.e., reliable UBV photometry, $T_{\rm eff}$, and $\log g$) does not exist in the literature. In order to assess the physical separations of the low mass companions in AU, an accurate distance is required. Combined with the near-infrared data, optical photometry and spectroscopy should allow a complete determination of stellar parameters for these binary and triple systems.

Stellar parameters are not only needed to determine distance and separation for these binaries, but also to study the system components themselves. Another goal of this survey is to compare the masses (via spectral types) of the red dwarf companions in wide, resolved systems versus those in unresolved, likely post-common envelope systems. Given enough stars in both categories, a statistical analysis can be made of the resulting spectral type (and, by proxy, mass) distributions to see what effect, if any, common envelope evolution has had on the secondary masses (Farihi 2004; Farihi et al. 2005)

J. Farihi would like to thank the following people for their much appreciated software and computing support directly related to this work: R. Hook, C. Hanley, D. Starr, K. Labrie, & K. Chiboucas. Sincere thanks goes to the anonymous refereee for many helpful comments which improved the quality of the manuscript. This work is based on observations made with the Hubble Space Telescope which is operated by the Association of Universities for Research in Astronomy under NASA contract NAS 5-26555. Support for Program number 10255 was provided by NASA through grant HST-GO-10255 from the Space Telescope Science Institute. Some data used in this paper are part of the Two Micron All Sky Survey, a joint project of the University of Massachusetts and the Infrared Processing and Analysis Center (IPAC)/CIT, funded by NASA and the National Science Foundation. 2MASS data were retrieved from the NASA/IPAC Infrared Science Archive, which is operated by the Jet Propulsion Laboratory, CIT, under contract with NASA. This research has made use of NASA's Astrophysics Data System Bibliographic Services, and the SIMBAD database, operated at CDS, Strasbourg, France.

Facility: HST (ACS)

REFERENCES

Bergeron, P., Leggett, S., & Ruiz, M. 2001, ApJS, 133, 413

Bergeron, P., Saffer, R., & Liebert, J. 1992, ApJ, 394, 228

Bergeron, P., Saumon, D., & Wesemael, F. 1995a, ApJ, 443, 764

Bergeron, P., Wesemael, F., & Beauchamp, A. 1995b, PASP, 107, 1047

Bleach, J., Wood, J., Smalley, B., & Catalán, M. 2002, MNRAS, 336, 611

Bond, H. 1985, Proceedings of the 7th N. American Workshop on Cataclysmic Variables and Low-Mass X-Ray Binaries, (Dordrecht: D. Reidel), 15

Bond, H., & Livio, M. 1990, ApJ, 355, 568

Bragaglia, A., Renzini, A., & Bergeron, P. 1995, ApJ, 443, 735

Catalán, M., Sarna, M., Jomaron, C., & Smith, R. 1995, MNRAS, 275, 153

Cooke, B., et al. 1992, Nature, 335, 61

Cutri, R., et al. 2003, 2MASS All Sky Catalog of Point Sources (IPAC/CIT)

Dahn, C., et al. 1982, AJ, 87, 419

Dahn, C., et al. 2002, AJ, 124, 1170

Darling, G., & Wegner, G., 1996, AJ, 111, 865

de Kool, M., & Ritter, H., 1993, A&A, 267, 397

Dreizler, S., & Werner K. 1996, A&A, 314, 217

Eggen, O., & Bessell, M. 1978, ApJ, 226, 411

Farihi, J. 2004, Ph.D. Thesis, UCLA

Farihi, J., Becklin, E., & Zuckerman, B. 2005, ApJS, 161, 394

Fleming, T., Snowden, S., Pfefferman, E., Briel, U., & Greiner, J. 1996, A&A, 316, 147

Finley, D., Koester, D., & Basri, G. 1997, ApJ, 488, 375

Ford, H., et al. 1998, SPIE, 3356, 234

Friedrich, S., Koester, D., Christlieb, N., Reimers, D., & Wisotzki, L., 2000,A&A363, 1040

Fuhrmeister, B., & Schmitt, J. 2003, A&A, 403, 247

Gizis, J. 1997, AJ, 113, 806

Green, P., Ali, B., & Napiwotzki, R. 2000, ApJ, 540, 992

Greenstein, J. 1974, ApJ, 189, L131

Greenstein, J. 1975, ApJ, 196, L117.

Greenstein, J. 1979, ApJ, 227, 244

Greenstein, J. 1984, ApJ, 276, 602

Greenstein, J. 1986, AJ, 92, 867

Hambly, N., Irwin, M., & MacGillivray, H. 2001, MNRAS, 326, 1295

Holberg, J., Barstow, M., & Burleigh, M. 2003, ApJS, 147, 145

Hutchings, J., Crampton, D., Cowley, A., Schmidtke, P., McGrath, T., & Chu, Y. 1995, PASP, 107, 931

Jeans, J. 1924, MNRAS, 85, 2

Jordan, S., & Heber, U. 1993, Proceedings of the 8^{th} European Workshop on White Dwarfs, ed. M. Barstow (Dordrecht: Kluwer), 403, 47

Kawka, A., Vennes, S., & Thorstensen, J. 2004, AJ, 127, 1702

Kirkpatrick, J., & McCarthy, D. 1994, AJ, 107, 333

Kleinman, S. et al. 2004, ApJ, 607, 426

Koester, D., et al. 2001, A&A, 378, 556

Lamontagne, R., Demers, S., Wesemael, F., Fontaine, G., & Irwin, M. 2000, AJ, 119, 241

Liebert, J., Bergeron, P., & Holberg, J. 2004, ApJS, 156, 47

Liebert, J., et al. 1994, ApJ. 421, 733

Livio, M., & Soker, N. 1984, MNRAS, 208, 783

Livio, M., & Soker, N. 1988, ApJ, 329, 764

Livio, M. 1996, ASP Conference Series 90: The Origins, Evolution, and Destinies of Binary Stars in Clusters, ed. E. Milone, J. Mermilliod, (San Francisco: ASP), 291

Marsh, T., Dhillon, V., & Duck, S. 1995, MNRAS, 275, 828

Marsh, M., et.al. 1997, MNRAS, 286,369

Maxted, P., Marsh, T., Moran, C., Dhillon, V., & Hilditch, R. 1998, MNRAS, 300, 1225

Maxted, P., Moran, C., Marsh, T., & Gatti, A. 2000, MNRAS, 311, 877

McCook, G., & Sion, E. 1999, ApJS, 121, 1

Monet, D., et al. 1998, The USNO-A2.0 Catalogue (U.S. Naval Observatory Flagstaff Station and Universities Space Research Association)

Monet, D., et al. 2003, AJ, 125, 984

Morales-Rueda, L., Marsh, T., Maxted, P., Nelemans, G., Karl, C., Napiwotzki, R., & Moran, C. 2005, MNRAS, 359, 648

Mueller, B., & Bues, I. MitAG, 70, 345

Napiwotzki, R., Green, P., & Saffer, R. 1999, ApJ, 517, 399

Oswalt, T., Peterson, B., & Foltz, C. 1984, AJ, 89, 421

Paczynski, B. 1976, Proceedings of IAU Symposium 73, eds. P. Eggleton, S. Mitton, & J. Whelan (Dordrecht: D. Reidel), 75

Probst, R. 1983, ApJS, 53, 335

Raymond, S., et al. 2003, AJ, 125, 2621

Reid, I. 1996, AJ, 111, 2000

Reid, I., & Hawley, S. 2000, in New Light on Dark Stars, (New York: Springer)

Saffer, R., Wade, R., Liebert, J., Green, R., Sion, E., Bechtold, J., Foss, D., & Kidder, K. 1993, AJ, 105, 1945

Schmidt, G., Smith, P., & Harvey, D. 1995, AJ, 110, 398

Schreiber, M., & Gänsicke, B. 2003, A&A, 406, 305

Schultz, G., Zuckerman, B., & Becklin E. 1996, ApJ, 460, 402

Silvestri, N., Oswalt, T., & Hawley, S. 2002, AJ, 124, 1118

Sion, E., Holberg, J., Barstow, M., & Kidder, K. 1995, PASP, 107, 232

Sirianni, M. et al. 2005, PASP, 117, 1049

Stepanian, J., Green, R., Foltz, C., Chaffee, F., Chavushyan, V., Lipovetsky, V., & Erastova, L. 2001, AJ, 122, 3361

Valls-Gabaud, E. 1988, Ap&SS, 142, 289

van den Besselaar, E., Roelofs, G., Nelemans, G., Augusteijn, T., & Groot, P. 2005, A&A, 434, L13

Vennes, S., Thejll, P., Galvan, R., & Dupuis, J. 1997, ApJ, 480, 714

Wachter, S., Hoard, D., Hansen, K., Wilcox, R., Taylor, H., & Finkelstein, S. 2003, ApJ, 586, 1356

Wegner, G., Africano, J., & Boodrich, B. 1990, AJ, 99, 1907

Wegner, G., McMahan, R., Boley, & Forrest I. 1987, AJ, 94, 1271

Wesemael, F., Green, R., & Liebert, J. 1985, ApJS, 58, 379

Williams, T., McGraw, J., & Grashuis, R. 2001, PASP, 113, 490

Yungelson, L., Tutukov, A., & Livio, M. 1993, ApJ, 418, 794

Zuckerman, B., & Becklin, E. 1987, ApJ, 319, 99

Zuckerman, B., & Becklin, E. 1987b, Nature, 330. 138

Zuckerman, B., & Becklin, E. 1992, ApJ, 386, 260

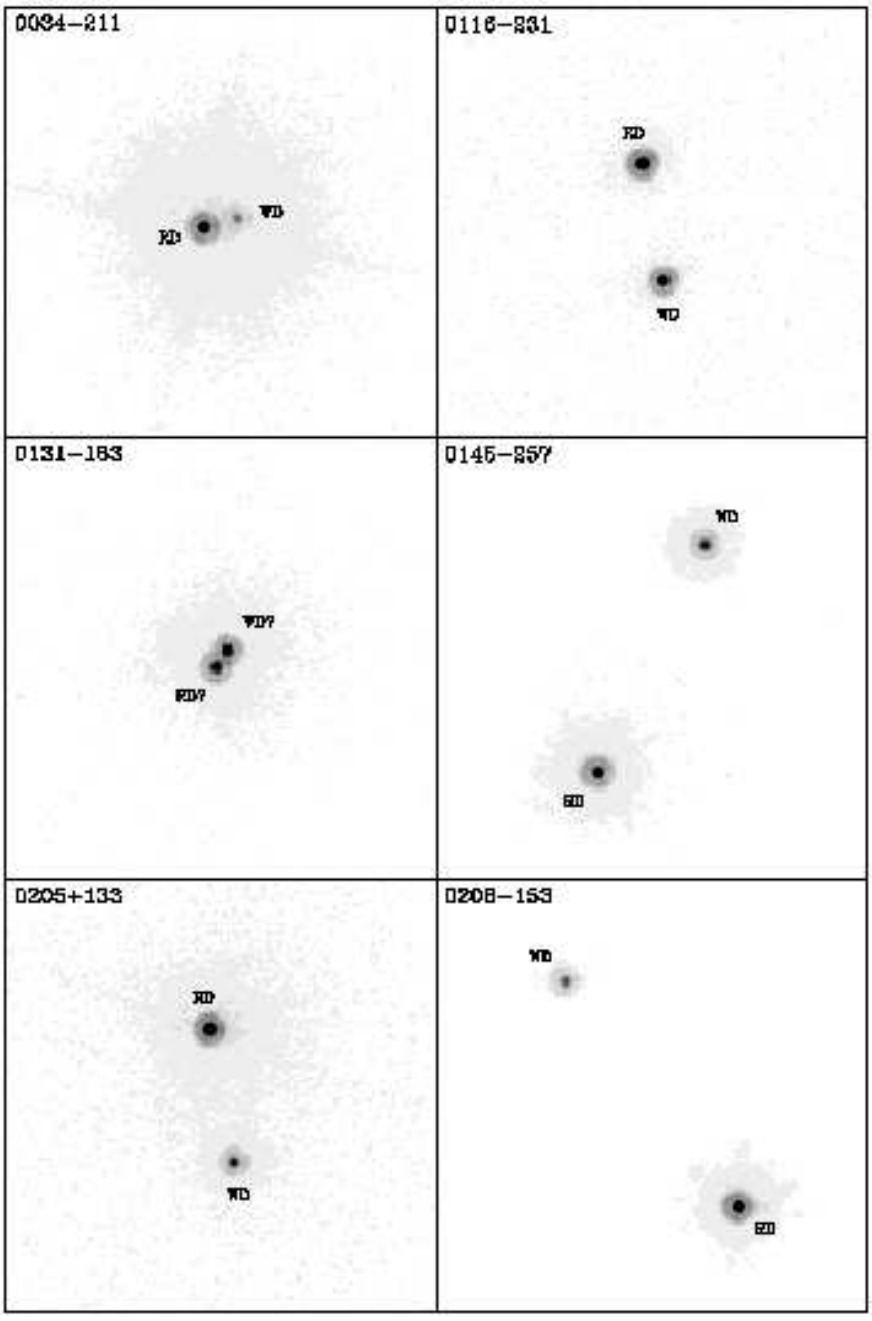

Fig. 1a.— Multidrizzled images of the ACS/HRC data taken in the F814W filter of all 28 totally or partially resolved multiple systems, plus an example of a single unresolved point source (0303−007). The images are $4'' \times 4''$ ($0.''025$ pixels) with North up and East left.

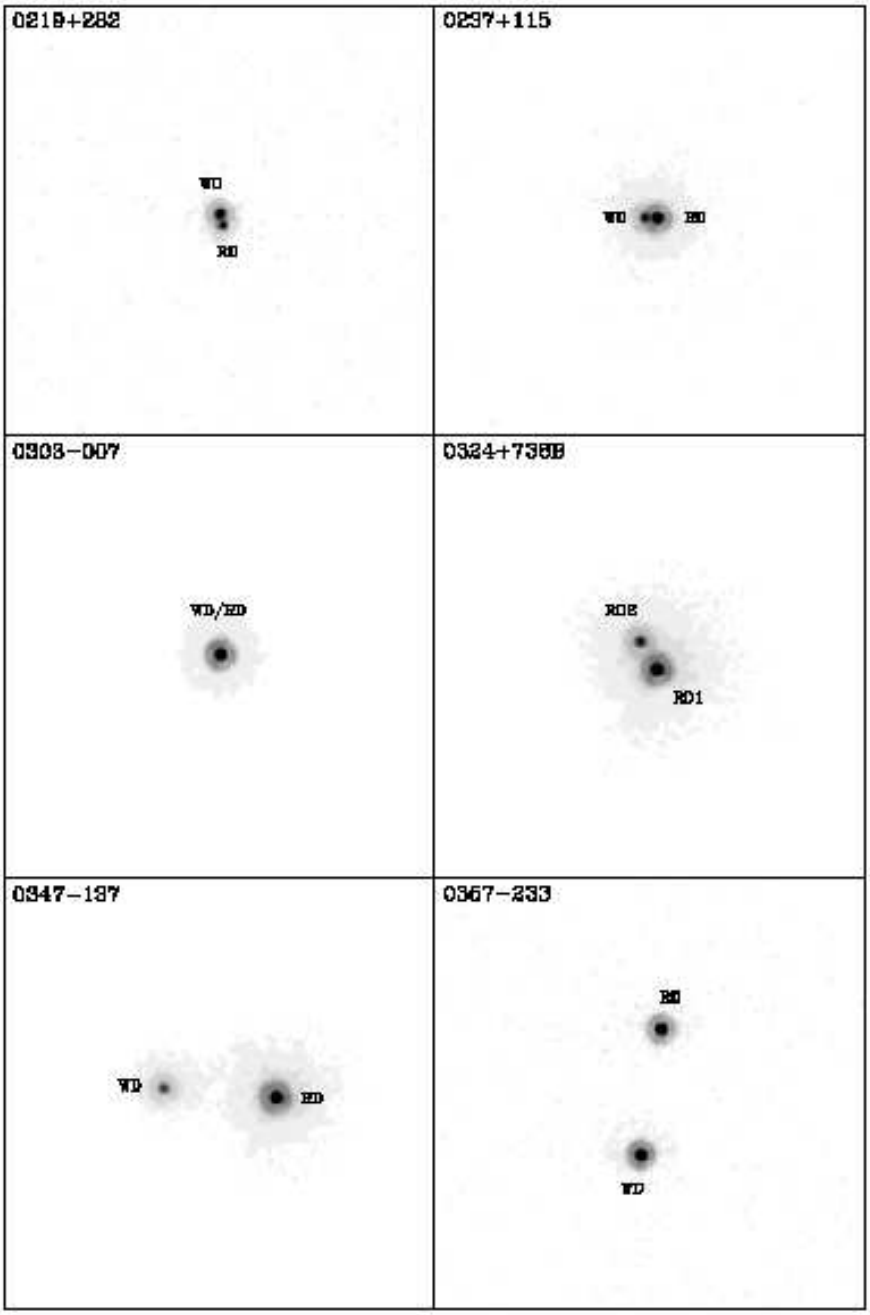

Fig. 1b.— see Figure 1a.

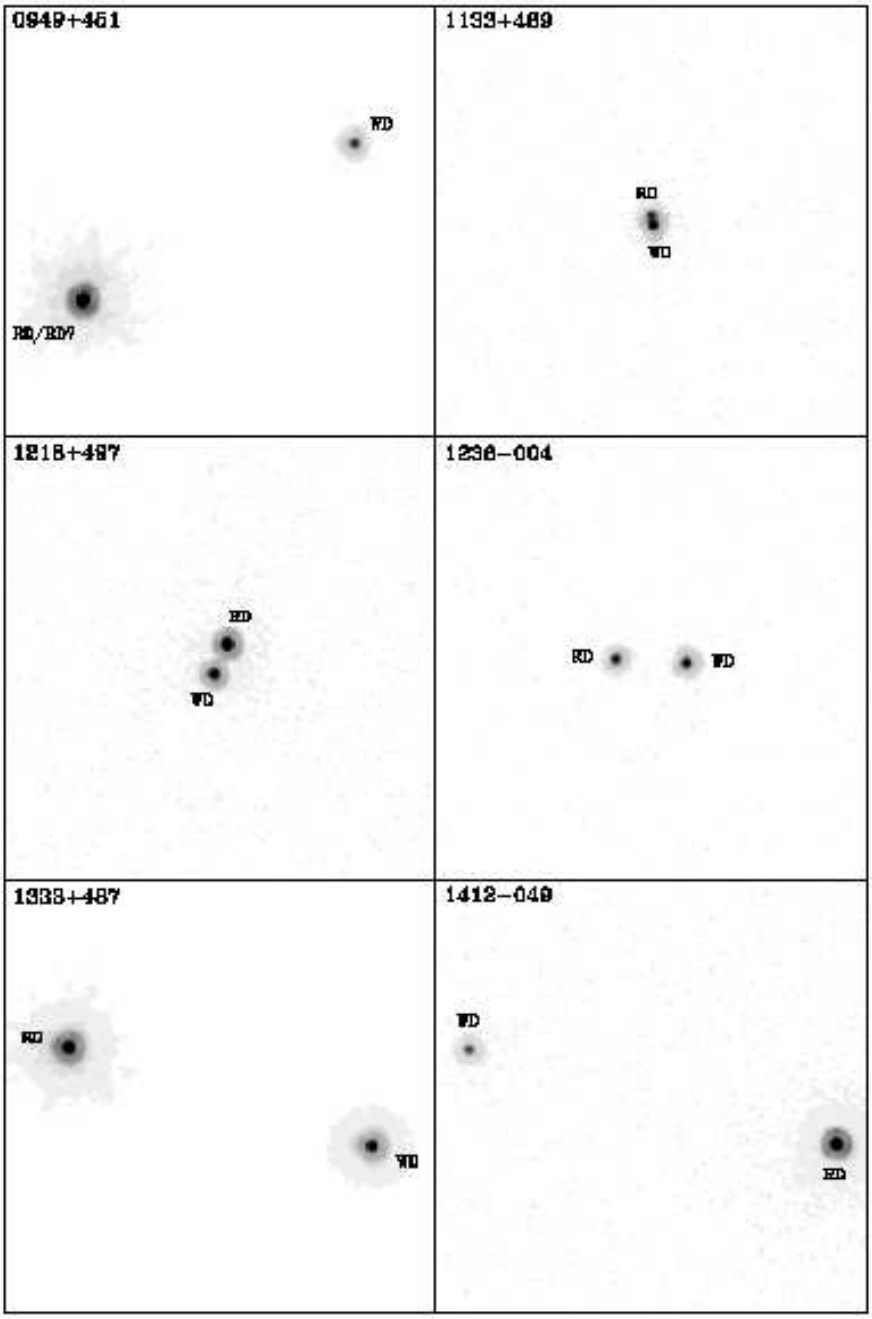

Fig. 1c.— see Figure 1a.

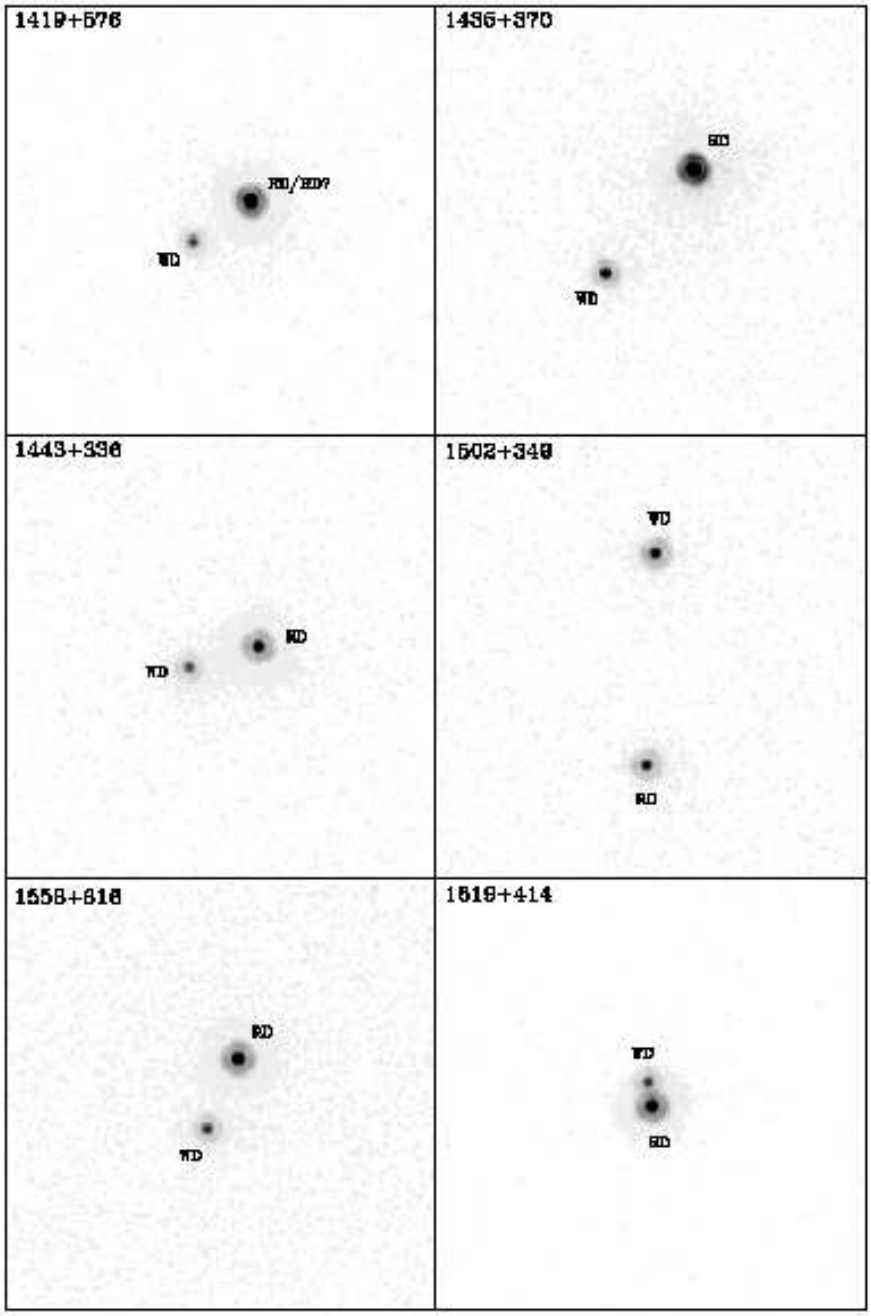

Fig. 1d.— see Figure 1a.

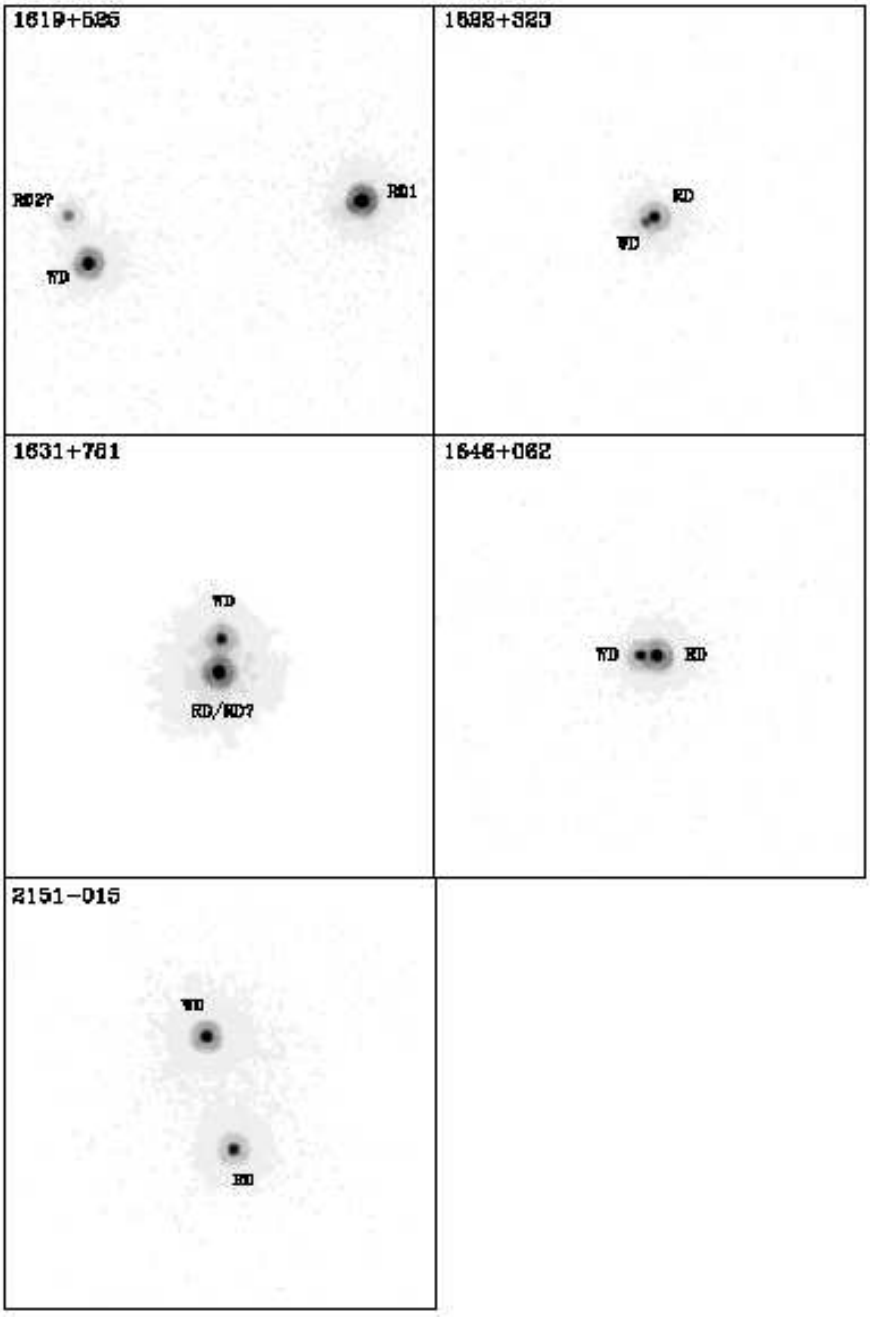

Fig. 1e.— see Figure 1a.

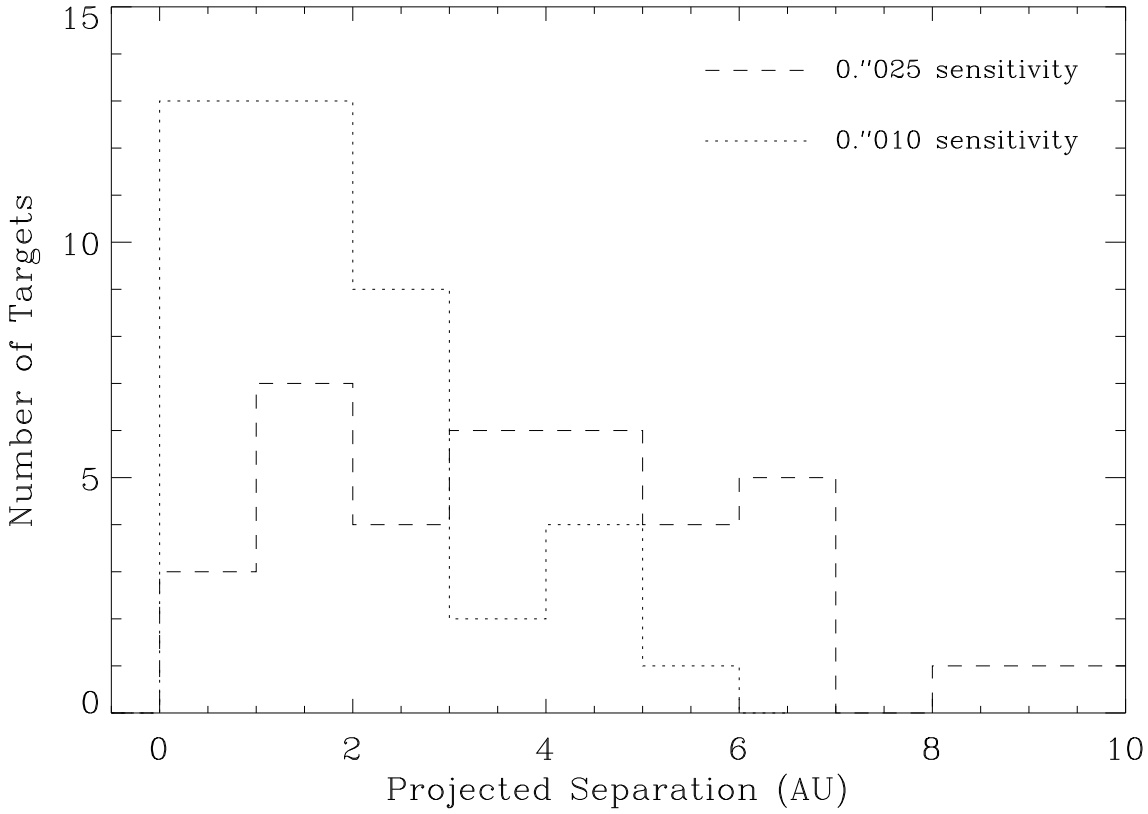

Fig. 2.— The number of targets from Tables 3 and 4 for which the ACS imaging data were sensitive to companion detection in the 0.3 AU (the minimum detectable projected separation) to 10 AU range. The bin size is 1 AU with integer bounds. The dashed line assumes a sensitivity of 0.″025 while the dotted line assumes 0.″010. All 41 bona fide white dwarf targets with strong evidence for near-infrared excess were sensitive to companion imaging detection within 5 AU, plus numerous targets sensitive to detections within 1 AU.

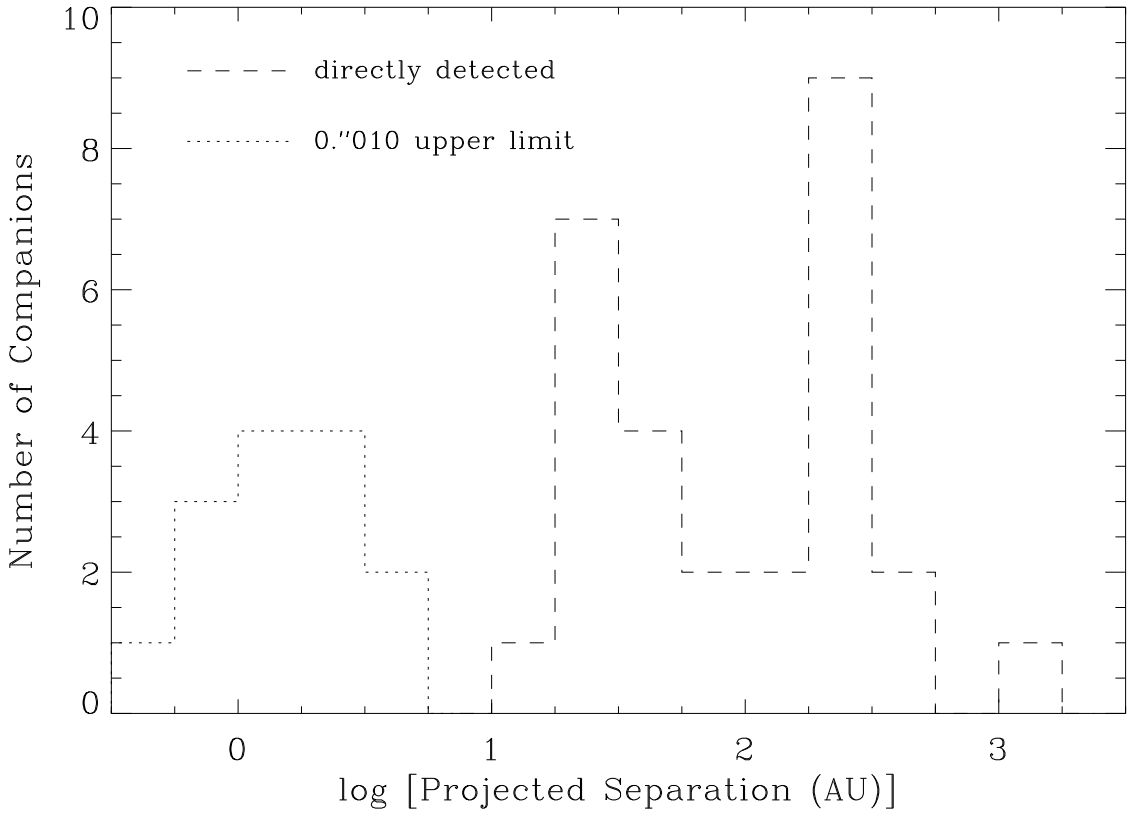

Fig. 3.— The distribution of projected separations for targets from Tables 3 and 4. The bin size is 0.25 in logarithmic units of AU, with identical bounds. The dashed line represents directly detected companions, while the dotted line represents upper limits of 0.″010 for those binaries which remained unresolved.

Table 1. Target ACS Data

WD#	Name	Resolved?	FWHM (″)	a/b	a_{sky} (″)	PA (°)	F814W (mag)†	I_c (mag)†	Notes
0023+388	G171-B10A	No	0.0747	1.030	···	···	15.18 ± 0.02	15.18 ± 0.03	1,6,7
0034−211	LTT 0329	Yes	0.0732	1.034	···	···	15.10 ± 0.04	15.07 ± 0.05	2,5
			0.0757	1.022	0.328 ± 0.002	106.04 ± 0.13	12.83 ± 0.02	12.89 ± 0.03	5
0116−231	GD 695	Yes	0.0733	1.006	···	···	16.60 ± 0.02	16.57 ± 0.03	2
			0.0754	1.019	1.105 ± 0.002	9.90 ± 0.04	16.16 ± 0.02	16.27 ± 0.03	
0131−163	GD 984	Yes	0.0745	1.017	···	···	14.28 ± 0.03	14.23 ± 0.04	2,5
			0.0751	1.017	0.189 ± 0.002	145.26 ± 0.23	14.49 ± 0.03	14.57 ± 0.04	5
0145−257	GD 1401	Yes	0.0740	1.017	···	···	14.98 ± 0.02	14.86 ± 0.03	2
			0.0761	1.011	2.295 ± 0.002	154.11 ± 0.02	13.83 ± 0.02	13.91 ± 0.03	
0205+133	PG	Yes	0.0737	1.044	···	···	15.44 ± 0.02	15.27 ± 0.03	2
			0.0762	1.040	1.257 ± 0.002	10.68 ± 0.03	13.91 ± 0.02	13.97 ± 0.03	
0208−153	MCT	Yes	0.0753	1.026	···	···	15.93 ± 0.02	15.90 ± 0.03	2
			0.0741	1.021	2.647 ± 0.002	217.39 ± 0.02	13.78 ± 0.02	13.83 ± 0.03	
0219+282	KUV	Yes	0.0750	1.032	···	···	17.33 ± 0.03	17.29 ± 0.04	2,5,16
			0.0773	1.086	0.117±0.005	195.2 ± 1.2	18.13 ± 0.06	18.29 ± 0.07	5
0237+115	PG	Yes	0.0756	1.046	···	···	16.35 ± 0.05	16.31 ± 0.06	2,5,14
			0.0760	1.020	0.124 ± 0.005	268.2 ± 1.2	15.01 ± 0.03	15.05 ± 0.04	5
0303−007	KUV	No	0.0758	1.024	···	···	14.54 ± 0.02	14.57 ± 0.03	1
0324+738	G221-10	No	0.0751	1.042	···	···	16.61 ± 0.02	16.60 ± 0.03	3,6,7,10
	G221-11	Yes	0.0767	1.028	···	···	13.68 ± 0.02	13.82 ± 0.03	2,5,19
			0.0760	1.037	0.297 ± 0.003	31.48 ± 0.29	15.11 ± 0.04	15.30 ± 0.05	5
0347−137	GD 51	Yes	0.0745	1.017	···	···	15.58 ± 0.02	15.55 ± 0.03	2
			0.0767	1.024	1.052 ± 0.002	265.16 ± 0.04	13.64 ± 0.02	13.71 ± 0.03	
0354+463	Rubin 80	No	0.0742	1.017	···	···	14.91 ± 0.02	14.90 ± 0.03	1
0357−233	Ton S 392	Yes	0.0745	1.017	···	···	16.22 ± 0.02	16.18 ± 0.03	2

Table 1—Continued

WD#	Name	Resolved?	FWHM (″)	a/b	a_{sky} (″)	PA (°)	F814W (mag)†	I_c (mag)†	Notes
			0.0755	1.014	1.190 ± 0.002	351.00 ± 0.04	16.46 ± 0.02	16.52 ± 0.03	
0458−662	WD	No	0.0750	1.021	···	···	14.56 ± 0.02	14.58 ± 0.03	1,9,11
0949+451	HS	Yes	0.0744	1.016	···	···	15.90 ± 0.02	15.89 ± 0.03	2,6
			0.0782	1.125	2.892 ± 0.002	119.66 ± 0.02	13.53 ± 0.04	13.58 ± 0.05	4
							14.3 ± 0.2	14.3 ± 0.2	8
					0.009 ± 0.005	350 ± 16	14.3 ± 0.2	14.3 ± 0.2	8
1051+516	SBS	No	0.0755	1.007	···	···	14.68 ± 0.02	14.70 ± 0.03	1,9
1133+489	PG	Yes	0.0740	1.030	···	···	17.53 ± 0.04	17.49 ± 0.05	2,5,14
			0.0756	1.076	0.094 ± 0.005	10.0 ± 1.5	18.18 ± 0.06	18.34 ± 0.07	5
1218+497	PG	Yes	0.0736	1.029	···	···	16.74 ± 0.02	16.70 ± 0.03	2,5
			0.0739	1.022	0.302 ± 0.002	335.22 ± 0.15	16.14 ± 0.02	16.21 ± 0.03	5
1236−004	WD	Yes	0.0747	1.031	···	···	17.93 ± 0.03	17.89 ± 0.04	2
			0.0756	1.015	0.658 ± 0.004	87.30 ± 0.17	18.05 ± 0.04	18.16 ± 0.05	
1247+550	LHS 342	No	0.0756	1.013	···	···	16.41 ± 0.02	16.43 ± 0.03	1,7,10,12
1333+005*	LP 618-14	No	0.0762	1.033	···	···	15.64 ± 0.02	15.73 ± 0.03	1,15
1333+487	GD 325	Yes	0.0747	1.020	···	···	14.24 ± 0.02	14.23 ± 0.03	2,13
			0.0764	1.015	2.947 ± 0.002	71.97 ± 0.02	13.39 ± 0.02	13.50 ± 0.03	
1339+606	RE	No	0.0738	1.026	···	···	16.48 ± 0.02	16.48 ± 0.03	1
1412−049	PG	Yes	0.0722	1.040	···	···	17.10 ± 0.03	17.06 ± 0.04	2
			0.0747	1.032	3.508 ± 0.002	255.53 ± 0.02	14.76 ± 0.02	14.82 ± 0.03	
1419+576	SBS	Yes	0.0741	1.019	···	···	17.54 ± 0.03	17.52 ± 0.04	2,6
			0.0778	1.114	0.658 ± 0.002	304.06 ± 0.15	15.05 ± 0.04	15.11 ± 0.05	4
							15.8 ± 0.2	15.9 ± 0.2	8
					0.008 ± 0.005	205 ± 18	15.8 ± 0.2	15.9 ± 0.2	8
1433+538	GD 337	No	0.0741	1.005	···	···	15.68 ± 0.02	15.69 ± 0.03	1

Table 1—Continued

WD#	Name	Resolved?	FWHM (″)	a/b	a_{sky} (″)	PA (°)	F814W (mag)†	I_c (mag)†	Notes
1435+370	CBS 194	Yes	0.0710	1.074	···	···	16.93 ± 0.02	16.89 ± 0.03	2
			0.0754	1.032	1.251 ± 0.002	318.80 ± 0.04	14.80 ± 0.02	14.85 ± 0.03	
1443+336	PG	Yes	0.0723	1.033	···	···	16.93 ± 0.02	16.89 ± 0.03	2
			0.0745	1.021	0.679 ± 0.002	286.17 ± 0.08	15.53 ± 0.02	15.60 ± 0.03	
1458+171	PG	No	0.0747	1.025	···	···	15.82 ± 0.02	15.81 ± 0.03	1,12
1502+349	CBS 223	Yes	0.0740	1.026	···	···	16.89 ± 0.02	16.84 ± 0.03	2
			0.0758	1.030	1.913 ± 0.002	179.31 ± 0.02	17.07 ± 0.03	17.16 ± 0.04	
1504+546	CBS 301	No	0.0741	1.039	···	···	15.02 ± 0.02	15.02 ± 0.03	1,9
1517+502	CBS 311	No	0.0735	1.040	···	···	16.69 ± 0.02	16.70 ± 0.03	1,17
1558+616	HS	Yes	0.0734	1.023	···	···	17.29 ± 0.03	17.27 ± 0.04	2
			0.0768	1.016	0.715 ± 0.002	336.26 ± 0.12	15.73 ± 0.02	15.82 ± 0.03	
1603+125	KUV	No	0.0726	1.044	···	···	14.15 ± 0.02	14.16 ± 0.03	1,18
1619+525	PG	Yes	0.0731	1.013	···	···	15.81 ± 0.02	15.79 ± 0.03	3,6
			0.0748	1.011	2.596 ± 0.002	282.52 ± 0.02	15.18 ± 0.02	15.28 ± 0.03	
			0.0756	1.040	0.466 ± 0.003	23.97 ± 0.16	17.85 ± 0.04	18.11 ± 0.05	
1619+414	KUV	Yes	0.0735	1.007	···	···	17.39 ± 0.03	17.36 ± 0.04	2,5
			0.0764	1.008	0.231 ± 0.002	188.79 ± 0.38	15.67 ± 0.02	15.74 ± 0.03	5
1622+323	PG	Yes	0.0730	1.079	···	···	16.93 ± 0.08	16.89 ± 0.10	2,5
			0.0747	1.066	0.094 ± 0.005	300.8 ± 1.5	15.78 ± 0.04	15.83 ± 0.05	5
1631+781	RE	Yes	0.0742	1.011	···	···	13.62 ± 0.03	13.58 ± 0.04	2,6,9
			0.0757	1.102	0.302 ± 0.002	355.87 ± 0.14	12.29 ± 0.04	12.36 ± 0.05	4
							13.0 ± 0.2	13.1 ± 0.2	8
					0.007 ± 0.005	200 ± 20	13.0 ± 0.2	13.1 ± 0.2	8
1646+062	PG	Yes	0.0734	1.025	···	···	16.46 ± 0.04	16.42 ± 0.05	2,5
			0.0744	1.036	0.163 ± 0.003	270.98 ± 0.53	15.40 ± 0.03	15.48 ± 0.04	5

Table 1—Continued

WD#	Name	Resolved?	FWHM (″)	a/b	a_{sky} (″)	PA (°)	F814W (mag)†	I_c (mag)†	Notes
1845+683	KUV	No	0.0732	1.015	···	···	15.65 ± 0.02	15.61 ± 0.03	1,7
2009+622	GD 543	No	0.0747	1.030	···	···	15.05 ± 0.02	15.06 ± 0.03	1,9,11
2151−015	LTT 8747	Yes	0.0733	1.023	···	···	14.30 ± 0.02	14.29 ± 0.03	2
			0.0776	1.024	1.082 ± 0.002	193.73 ± 0.04	15.07 ± 0.02	15.34 ± 0.03	
2211+372	LHS 3779	No	0.0735	1.010	···	···	16.38 ± 0.02	16.38 ± 0.03	1,7,10
2237−365	LHS 3841	No	0.0750	1.010	···	···	14.83 ± 0.02	14.93 ± 0.03	1,15
2317+268	KUV	No	0.0749	1.026	···	···	15.64 ± 0.02	15.61 ± 0.03	1
2323+256	G128-62	No	0.0739	1.027	···	···	16.29 ± 0.02	16.29 ± 0.03	1,7,10
2349−283	GD 1617	No	0.0734	1.010	···	···	15.65 ± 0.02	15.62 ± 0.03	1,7

Note. — (1) Single point source; (2) Double point source, two Airy disks; (3) Triple point source, three Airy disks (4) Single elongated Airy disk; (5) Measurements affected by close binarity; (6) Triple system; (7) Low S/N in 2MASS; (8) Equal luminosity assumed; (9) DA+dMe; (10) Cool red WD, $T_{\rm eff} < 8000$ K; (11) Radial velocity variable; (12) low mass, He core WD; (13) DB+dM; (14) DO+dM; (15) DC+dM; (16) DBA+dM; (17) DA+dC; (18) sdB+dK; (19) Common proper motion companion

*Not in McCook & Sion (1999), WD# unofficial

†All photometry is in Vega magnitudes. Photometric and astrometric errors are discussed in §3.1.

Table 2. White Dwarf Parameters

WD#	$T_{\rm eff}$ (K)	log g	V (mag)	$d_{\rm wd}$ (pc)	References
0023+388	10,400	8.0	15.97	62	1,13
0034−211	17,200	8.04	15.03	63	1,4,5,14,15
0116−231	25,000	7.9	16.29	164	1,16,17
0131−163	50,000	7.75	13.90	109	1,3,6,7,8,9
0145−257	26,200	7.93	14.59	78	1,6,7
0205+133	57,400	7.63	15.04	221	1,2,3
0208−153	25,000	7.9	15.64	122	1,2
0219+282	25,000	7.9	17.03	231	1,19
0237+115	70,000	8.00	15.96	272	1,8,20
0303−007	17,000	8.0	16.48	126	1,11
0324+738	7200	8.4	17.05	40	1,3,21
0347−137	21,300	8.27	15.32	71	1,4,5,10
0354+463	8000	8.0	15.58	33	1,4,5
0357−233	50,000	7.8	15.93	278	1,4,5,22
0458−662	20,000	7.9	17.72	258	1,23
0949+451	14,000	8.0	15.77	77	1,24
1051+516	20,000	7.9	17.00	185	1,12
1133+489	47,500	7.8	17.08	429	1,18
1218+497	35,700	7.87	16.39	254	1,2
1236−004	34,000	7.9	17.58	437	1,25
1247+550	4050	7.57	17.79	25	26
1333+005	8500	8.0	17.46	87	1,4,5
1333+487	14,000	8.0	14.10	35	1,27
1339+606	43,000	7.68	16.94	402	1,28
1412−049	40,000	7.8	16.74	333	1
1419+576	35,000	7.9	17.22	373	1,12
1433+538	22,400	7.80	16.12	151	1,3,4,5
1435+370	25,000	7.9	16.63	192	1,3
1443+336	29,800	7.83	16.59	278	1,2
1458+171	22,000	7.43	16.30	216	1,2
1502+349	20,000	7.9	16.62	156	1

Table 2—Continued

WD#	$T_{\rm eff}$ (K)	log g	V (mag)	$d_{\rm wd}$ (pc)	References
1504+546	25,000	7.9	16.20	158	1
1517+502	31,100	7.84	17.80	413	1,12,29
1558+616	25,000	7.9	17.01	229	1
1603+125	···	···	15.6	1660	1,11
1619+525	18,000	7.90	15.60	93	1,2
1619+414	20,000	7.9	17.14	198	1,11
1622+323	68,300	7.56	16.55	520	1,2
1631+781	39,900	7.88	13.21	57	1,4,5,8
1646+062	29,900	7.98	16.12	175	1,2
1845+683	37,000	8.21	15.30	116	1,6,7,9
2009+622	25,900	7.70	15.26	134	1,4,5,30
2151−015	8500	8.0	14.41	21	1,3,4,5
2211+372	6300	8.0	16.70	50	3,33
2237−365	7200	8.0	17.25	59	1,31
2317+268	25,000	7.9	16.54	185	1,32
2323+256	6000	8.0	17.06	37	1,3
2349−283	17,300	7.73	15.44	90	1,10

Note. — A single digit following the decimal place for log g indicates an assumption of $M = 0.60\ M_{\odot}$. V magnitudes are uncontaminated or rederived values based on effective temperature and models, magnitudes and colors in other filters, or photographic magnitudes and colors (see §3.6). Absolute magnitudes come from the models of Bergeron et al. (1995a,b) as well as the specified references.

References. — (1) This work; (2) Liebert et al. 2005; (3) McCook & Sion 1999; (4) Farihi 2004; (5) Farihi et al. 2005; (6) Finley et al. 1997; (7) Vennes et al. 1997; (8) Green et al. 2000; (9) Napiwotzki

et al. 1999; (10) Koester et al. 2001; (11) Wegner et al. 1990; (12) Stepanian et al. 2001; (13) Silvestri et al. 2002; (14) Bragaglia et al. 1995; (15) Greenstein 1974; (16) Lamontagne et al. 2000; (17) Eggen & Bessell 1978; (18) Wesemael et al. 1985; (19) Darling & Wegner 1996; (20) Dreizler & Werner 1996; (21) Greenstein 1984; (22) Greenstein 1979; (23) Hutchings et al. 1996; (24) Jordan & Heber 1993; (25) Kleinman et al. 2004; (26) Bergeron et al. 2001; (27) Dahn et al. 1982; (28) Marsh et al. 1997; (29) Liebert et al. 1994; (30) Bergeron et al. 1992; (31) Friedrich et al. 2000; (32) Oswalt et al. 1984; (33) Kawka et al. 2004

Table 3. Parameters of Resolved Secondary & Tertiary Stars

Primary	Companion	SpT	$I-K$	$d_{\rm rd}$ (pc)	Ref
0034−211	LTT 0329B	dM3.5	2.24	51	1,2,3,4,7,13
0116−231	GD 695B	dM4.5	2.39	171	1,2,14,15
0131−163	GD 984B	dM3.5	2.24	110	1,2,3,4,6,7
0145−257	GD 1401B	dM3.5	2.29	79	1,2,6,16
0205+133	PG 0205+133B	dM1	1.98	212	1,2,5,17
0208−153	WD 0208−153B	dM2	2.05	143	1,2
0219+282	KUV 0219+282B	dM5.5	2.87	231	1,2
0237+115	PG 0237+115B	dM3	2.14	211	1,5,10,19
0324+738	G221-11A	dM5	2.65	40	1
	G221-11B	dM6	3.19	40	1
0347−137	GD 51B	dM4.5	2.40	52	1,3,4
0357−233	Ton S 392B	dM3	2.17	410	1,3,4
0949+451	HS 0949+451B	dM4.5	2.53	66	1,9
	HS 0949+451C	dM4.5	2.53	66	1,9
1133+489	PG 1133+489B	dM5	2.83	327	1,5,18
1218+497	PG 1218+497B	dM4	2.33	164	1,2,5,10
1236−004	WD 1236−004B	dM4	2.56	363	1,2,20
1333+487	GD 325B	dM5	2.53	35	1,21
1412−049	PG 1412−049B	dM0	1.82	378	1,2
1419+576	SBS 1419+576B	dM2	2.00	374	1,8
	SBS 1419+576C	dM2	2.00	374	1,8
1435+370	CBS 194B	dM2.5	2.09	192	1,2
1443+336	PG 1443+336B	dM2.5	2.05	277	1,2
1502+349	CBS 223B	dM5	2.78	194	1,2
1558+616	HS 1558+616B	dM4.5	2.43	136	1,2,12
1619+525	PG 1619+525B	···	···	93	1,2
	PG 1619+525C	···	···	93	1,2
1619+414	KUV 1619+414B	dM5	2.70	105	1,2,22
1622+323	PG 1622+323B	dM1	2.03	488	1,2,5
1631+781	RE 1631+781B	dM3	2.18	85	1,2,3,4,6,7,11
	RE 1631+781C	dM3	2.18	85	1,2,3,4,6,7,11

Table 3—Continued

Primary	Companion	SpT	$I-K$	$d_{\rm rd}$ (pc)	Ref
1646+062	PG 1646+062B	dM3.5	2.21	170	1,5
2151−015	LTT 8747B	dM8	3.85	20	1,3,4

References. — (1) This work; (2) Wachter et al. 2003; (3) Farihi 2004; (4) Farihi et al. 2005; (5) Greenstein 1986; (6) Green et al. 2000; (7) Schultz et al. 1996; (8) Stepanian et al. 2001; (9) Jordan & Heber 1993; (10) Wesemael et al. 1985; (11) Cooke et al. 1992; (12) McCook & Sion 1999; (13) Probst 1983; (14) Eggen & Bessell 1978; (15) Lamontagne et al. 2000; (16) Mueller & Bues 1987; (17) Williams et al. 2001; (18) van den Besselaar et al. 2005; (19) Dreizler & Werner 1996; (20) Kleinman et al. 2004; (21) Greenstein 1975; (22) Wegner et al. 1990

Table 4. Unresolved Secondary Parameters

Primary	Companion	SpT	$I-K$	d (pc)	Ref
0023+388	G171-B10C	dM5.5	2.83	76	1,2,6
0303−007	KUV 0303−007B	dM4	2.32	84	1,2,7
0354+463	Rubin 80B	dM7	3.47	41	1,3,4,5
0458−662	WD 0458−662B	dM2.5	2.12	171	1,8
1051+516	SBS 1051+516B	dM3	2.20	183	1,2
1333+005	LP 618-14B	dM4.5	2.52	147	1,3,4,5
1339+606	RE 1339+606B	dM4	2.36	259	1,9
1433+538	GD 337B	dM5	2.54	162	1,3,4,5,10
1458+171	PG 1458+171B	dM5	2.72	156	1,2
1504+546	CBS 301B	dM4	2.33	112	1,2,11
1517+502	CBS 311B	dC	2.87	413	1,2,12
1603+125	KUV 1603+125B	dK3	1.38	1660	1,2
2009+622	GD 543B	dM4.5	2.51	156	1,3,4,5,13,14
2237−365	LHS 3841B	dM2	1.89	282	1,2
2317+268	KUV 2317+268B	dM3.5	2.23	219	1,2

References. — (1) This work; (2) McCook & Sion 1999; (3) Wachter et al. 2003; (4) Farihi 2004; (5) Farihi et al. 2005; (6) Reid 1996; (7) Wegner et al. 1987; (8) Hutchings et al. 1996; (9) Fleming et al. 1996; (10) Greenstein 1975; (11) Stepanian et al. 2001; (12) Liebert et al. 1994; (13) Greenstein 1984; (14) Morales-Rueda et al. 2005

Table 5. Projected Separations for All Double Stars

Binary	$a_{sky}(''$)	$a^{\dagger}$ (AU)	Type
0023+388AC	< 0.025	< 1.6	WD+RD
0034−211AB	0.328	21	WD+RD
0116−231AB	1.105	180	WD+RD
0131−163AB	0.189	21	WD+RD
0145−257AB	2.295	180	WD+RD
0205+133AB	1.257	280	WD+RD
0208−153AB	2.647	320	WD+RD
0219+282AB	0.117	27	WD+RD
0237+115AB	0.124	34	WD+RD
0303−007AB	< 0.025	< 3.2	WD+RD
0324+738BC	0.297	12	RD+RD
0347−137AB	1.052	75	WD+RD
0354+463AB	< 0.025	< 0.8	WD+RD
0357−233AB	1.190	330	WD+RD
0458−662AB	< 0.025	< 8.3	WD+RD
0949+451AB	2.892	220	WD+RD
0949+451BC	0.009	0.7	RD+RD
1051+516AB	< 0.025	< 4.6	WD+RD
1133+489AB	0.094	28	WD+RD
1218+497AB	0.302	77	WD+RD
1236−004AB	0.658	29	WD+RD
1333+005AB	< 0.025	< 2.2	WD+RD
1333+487AB	2.947	100	WD+RD
1339+606AB	< 0.025	< 10	WD+RD
1412−049AB	3.508	1200	WD+RD
1419+576AB	0.658	250	WD+RD
1419+576BC	0.008	3.0	RD+RD
1433+538AB	< 0.025	< 3.8	WD+RD
1435+370AB	1.251	240	WD+RD
1443+336AB	0.679	190	WD+RD
1458+171AB	< 0.025	< 5.4	WD+RD

Table 5—Continued

Binary	$a_{sky}(''$)	$a^{\dagger}$ (AU)	Type
1502+349AB	1.913	300	WD+RD
1504+546AB	< 0.025	< 4.0	WD+RD
1517+502AB	< 0.025	< 10	WD+RD
1558+616AB	0.715	160	WD+RD
1603+125AB	< 0.025	< 42	SD+RD
1619+525AB	2.596	240	WD+RD
1619+525AC	0.466	43	WD+RD
1619+414AB	0.231	46	WD+RD
1622+323AB	0.094	49	WD+RD
1631+781AB	0.302	17	WD+RD
1631+781BC	0.007	0.4	RD+RD
1646+062AB	0.163	29	WD+RD
2009+622AB	< 0.025	< 3.4	WD+RD
2151−015AB	1.082	23	WD+RD
2237−365AB	< 0.025	< 1.5	WD+RD
2317+268AB	< 0.025	< 4.6	WD+RD

†Values are the current projected separations, not the true length of the semimajor axes, and are based upon the photometric distance to the white dwarf (§3.6).